A broad-host range CRISPRi toolkit for silencing gene expression in Burkholderia

Short Title: CRISPRi toolkit for Burkholderia

Category: Microbiology

Andrew M. Hogan[1], A. S. M. Zisanur Rahman[1], Tasia J. Lightly[1] , Silvia T. Cardona[1,2*].

[1]Department of Microbiology, University of Manitoba, Winnipeg, MB, Canada.

[2]Department of Medical Microbiology & Infectious Disease, University of Manitoba, Winnipeg, Canada.

*To whom correspondence should be addressed: Silvia.Cardona@umanitoba.ca

Keywords: CRISPR-interference, *Burkholderia*, gene silencing, genetic tool

Abstract

Genetic tools are critical to dissecting the mechanisms governing cellular processes, from fundamental physiology to pathogenesis. Species of *Burkholderia* have emerged over recent decades as both important opportunistic pathogens in immunocompromised patients and as a rich source of secondary metabolites for biotechnology. With large, high GC content genomes, there are limited tools available for genetic manipulation of *Burkholderia* species. To address this, we have developed CRISPR interference (CRISPRi) technology for gene silencing in *Burkholderia*. Tunable expression was provided by placing a codon-optimized *dcas9* from *Streptococcus pyogenes* under control of a rhamnose-inducible promoter, which was validated by immunoblot. Expression from a multicopy plasmid caused a growth defect; therefore, the mini-CTX single-copy insertion system was used to deliver *dcas9* to the chromosome, resulting in wild-type growth. As a proof of concept, the *paaABCDE* operon controlling genes necessary for phenylacetic acid degradation was targeted by plasmid-borne sgRNAs, resulting in near complete inhibition of growth on phenylacetic acid as a sole carbon source. The utility of CRISPRi to probe other functions at the single cell level was demonstrated knocking down *phbC* and *fliF,* which dramatically reduces polyhydroxybutyrate granule accumulation and motility, respectively. As a hallmark of the mini-CTX system is the broad host-range of integration, we putatively identified 67 genera of Proteobacteria that might be amenable to modification with our CRISPRi toolkit.

Significance statement

Members of the genus *Burkholderia* have potential for biotechnological applications but can also cause disease in humans with a debilitated immune system. The lack of suitable genetic tools to edit *Burkholderia* GC-rich genomes has hampered the exploration of useful capacities and the understanding of pathogenic features. Our CRISPRi tool kit provides a simple and rapid way to silence gene expression to produce an observable phenotype. Linking genes to functions with CRISPRi will facilitate genome editing with the goal of enhancing biotechnological capabilities while reducing *Burkholderia's* pathogenic arsenal.

Author contributions

STC conceived the idea and design of the research; AMH designed and cloned the dCas9 constructs; AMH and ASMZ designed the sgRNAs, assessed knockdown phenotypes, processed data, and wrote and edited the manuscript; TJL performed qRT-PCR analysis and edited the manuscript; STC supervised the work and provided financial support.

Introduction

The genus *Burkholderia* comprises a diverse group of Gram-negative bacteria characterized by a remarkable biotechnological potential, with species that can be exploited for bioremediation purposes, production of bioactive compounds, and agricultural growth promotion. Perhaps due to the phylogenetic diversity of the genus, some species of *Burkholderia* can also pose a threat to human health (Eberl and Vandamme, 2016). Within the multiple deep-branching groups of the *Burkholderia* phylogenetic tree (Depoorter et al., 2016), one branch contains the clades known as the *Burkholderia cepacia* complex (Bcc) and the *B. pseudomallei* group. The Bcc group comprises species that cause severe infections in people with the genetic disease cystic fibrosis and other patients with a compromised immune system (Mahenthiralingam et al., 2005). *B. cenocepacia* and *B. multivorans* are two relevant species of this group, which are prevalent in cystic fibrosis patients (Kenna et al., 2017). The *B. pseudomallei* group contains the risk group 3 members *B. mallei*, *B. pseudomallei*, and its close relative *B. thailandensis*, the last one being a frequent surrogate used in *B. pseudomallei* and *B. mallei* research (Howe et al., 1971). Other branches, such as the *B. xenovorans* group comprise species isolated from diverse environmental sources, like polluted soils, and plant rhizospheres (Depoorter et al., 2016). While species with and without pathogenic potential tend to cluster separately in most phylogenetic trees, the genetic characteristics that define the pathogenic potential of *Burkholderia* are poorly understood. Environmental species can cause serious infections (Nally et al., 2018), calling for caution in the use of *Burkholderia* strains for biotechnological applications. The incomplete understanding of *Burkholderia* pathogenic potential may be related to the limited tools available to link gene to function. Most genome editing methods designed for Gram-negative bacteria are inefficient in

79 *Burkholderia* due in part to their high resistance to the antibiotics used as genetic markers (Rhodes
80 and Schweizer, 2016), and the high GC content of their large genomes.

81 Tools that facilitate controlled gene expression are necessary for interrogation of gene
82 function. Programmable control of gene expression by promoter replacement is a valuable tool to
83 link gene to phenotype (Judson and Mekalanos, 2000). Yet, promoter replacement implies that the
84 natural regulatory circuitry of the target gene is interrupted. Instead, clustered regularly interspaced
85 short palindromic repeats interference (CRISPRi) (Qi et al., 2013) is a method of silencing native
86 gene expression, which is based on a dead Cas9 (dCas9), a nuclease-inactive version of the RNA-
87 guided endonuclease Cas9 (Cho et al., 2013). In CRISPRi, a single guide RNA (sgRNA) designed
88 towards the 5' end of the target gene and the dCas9 protein form an RNA-protein complex that
89 recognizes the target region by base-pairing, and sterically blocks transcription initiation, if
90 targeting the promoter, or elongation if targeting downstream of the promoter, by the RNA
91 polymerase (Figure 1A).

92 Initially developed in *Escherichia coli*, CRISPRi technology has been applied to
93 functionally characterize genomes of a handful of bacteria (Lee et al., 2019; Liu et al., 2017; Peters
94 et al., 2016). To achieve genome-wide control of gene expression a wide range of dCas9 expression
95 levels are necessary, which can be provided by expressing *dcas9* with strong inducible promoters
96 (Peters et al., 2016) or by providing multiple copies of *dcas9* engineered in a plasmid (Lee et al.,
97 2019). Limitations to the success of these genomic efforts are the proteotoxicity of dCas9 when
98 expressed at high levels (Cui et al., 2018) and the necessity of customizing CRISPRi delivery tools
99 across bacteria. Recently, the use of Tn7 transposon mutagenesis, which specifically delivers
100 genetic constructs close to a single *glmS* site (Choi and Schweizer, 2006; Choi et al., 2005) was
101 applied to deliver a mobile CRISPRi system across bacteria (Peters et al., 2019). However, the

Tn7 system is less suitable for Burkholderia species as their genomes contain multiple copies of *glmS*, requiring additional steps to confirm the site of chromosomal integration (Choi et al., 2006).

In this work, we employ a mini-CTX-derived mutagenesis system (Hoang et al., 2000) to achieve specific chromosomal delivery of *dcas9* in three species of *Burkholderia*, *B. cenocepacia*, *B. thailandensis* and *B. multivorans*. Placing the chromosomal copy of *dcas9* under the control of the *E. coli* rhamnose-inducible promoter (Cardona and Valvano, 2005), we demonstrate durable and tunable control of endogenous gene expression, which affects cellular function producing observable phenotypes. We extend the usability of our CRISPRi tool kit by exploring other bacterial genomes for putative mini-CTX insertion sites.

Results

Construction of CRISPRi system

The dCas9 from *Streptococcus pyogenes* has been shown to provide robust gene repression in diverse bacteria (Peters et al., 2016, 2019; Qi et al., 2013); we therefore selected it as our first approach. To function, the dCas9 binds a sgRNA and, by complementary base pairing, is guided to target and silence a gene of interest by sterically blocking the RNA polymerase (Figure 1A) (Qi et al., 2013). However, the genome of *S. pyogenes* has low GC-content (~40%), and from inspection of the *dcas9* gene, we expected poor codon usage in high GC-content organisms such as *Burkholderia* (67%) and subsequently low levels of expression. Indeed, we did not observe detectable levels of dCas9 by immunoblot upon expression of the native gene from *S. pyogenes* from a single copy in the *B. cenocepacia* K56-2 chromosome (Supplemental Figure 1). Upon codon optimization for *B. cenocepacia*, we first introduced the gene into a multicopy plasmid

under the control of the rhamnose-inducible promoter (Cardona and Valvano, 2005); however, we observed a severe growth defect upon induction, except at minute concentrations of rhamnose (Supplemental Figure 2A). Growth inhibition was not observed in the vector control (Supplemental Figure 2B) and it remains unclear if the inhibitory effect of dCas9 expression on growth was caused by metabolic load from expression of a large protein in multicopy, or from proteotoxicity.

We reasoned a single chromosomal copy of *dcas9* may provide sufficient levels of expression as observed previously (Choudhary et al., 2015; Peters et al., 2016, 2019). Using the mini-CTX system, we introduced a single copy of *dcas9* under control of the rhamnose-inducible promoter into *B. cenocepacia* K56-2 (Supplemental Figure 3A and B). We observed titratable dCas9 expression at various levels of rhamnose by immunoblot (Figure 1B and Supplemental Figure 4A). At rhamnose concentrations up to 0.2% there was no growth defect (Figure 1C) compared to the vector control mutant (Supplemental Figure 4B) Furthermore, dCas9 expression in the presence of a sgRNA with a randomized binding region (sgRNA-non-target) had no effect on growth (Supplemental Figure 4C), demonstrating the current system is well-tolerated in *B. cenocepacia* K56-2.

Tunable and durable CRISPRi silencing of paaA strongly suppresses growth on phenylacetic acid

To evaluate the utility of the CRISPRi system for gene repression in *B. cenocepacia* K56-2, we first chose to target the *paaA* gene, which encodes phenylacetate-CoA oxygenase subunit PaaA (Teufel et al., 2010). This gene, and the rest of the *paaABCDE* operon, enable growth with PA as a sole carbon source in *B. cenocepacia* K56-2 (Pribytkova et al., 2014), with the lack of growth being a clearly observable phenotype when the *paaA* gene is disrupted. In addition, as this is the first characterization of CRISPRi in *Burkholderia*, we also wished to assess the effect on

147 repression efficiency when targeting the non-template (NT) and template (T) strands, as previous
148 studies have demonstrated profound differences (Bikard et al., 2013; Qi et al., 2013). We therefore
149 designed five sgRNAs: three sgRNAs targeted the promoter elements and adjacent to the
150 transcription start site (TSS) on the NT strand (sgRNA 1, 2 and 3), one sgRNA targeted near the
151 start codon of *paaA* on the NT strand (sgRNA 4), and one sgRNA targeted near the start codon of
152 *paaA* on the T strand (sgRNA 5) (Figure 2A). For phenotypic characterization of the *paaA* mutants,
153 we used M9 minimal medium with PA (M9+PA) as the sole carbon source. Upon induction of
154 dCas9, the growth of all mutants (except the controls) was suppressed approximately 30-fold
155 (Figure 2B) to the same level of a Δ*paaABCDE* mutant, which is unable to utilize PA as a sole
156 carbon source (Pribytkova et al., 2014). Furthermore, in the absence of rhamnose all of the mutants
157 grew at or near wild-type levels, suggesting that *dcas9* expression is tightly repressed in non-
158 inducing conditions. Interestingly, we did not observe a differential effect of placement of the
159 sgRNA-binding site, as the growth of all mutants was suppressed equally. We also found there to
160 be no difference in control strains; mutants expressing dCas9 and either a guideless or non-
161 targeting sgRNA displayed the same levels of growth.

162 Next, we sought to determine the tunability of our CRISPRi system in *Burkholderia*.
163 Tuning is useful to control the level of transcription inhibition when precision is required, such as
164 in the study of essential genes. To that end, we examined the growth of the dCas9 mutant of *B.*
165 *cenocepacia* K56-2 with the sgRNA1 (targeting *paaA*), using PA as a sole carbon source in the
166 presence of a 2-fold serial dilution of rhamnose. The results showed that our CRISPRi system is
167 tunable, exhibiting growth reduction in a dose-dependent manner with variable repression across
168 sub-saturating rhamnose concentrations (Figure 2C). Intermediate levels of growth were observed
169 in concentrations of rhamnose between 0.00625% and 0.05%. We observed a nearly 30-fold

repression in OD_{600nm} at concentrations well below maximum induction as identified by immunoblot, suggesting our system produces more dCas9 than is required for maximum repression. Rhamnose levels beyond 0.2% were intrinsically growth inhibitory precluding their use for inducing gene expression (Figure 2C).

Although once rhamnose is removed from the culture, expression of dCas9 is no longer induced, it remained possible that the dCas9 already synthesized may persist and cause long-term, or durable, silencing. To address this, the mutant strains harbouring sgRNAs targeting *paaA,* were grown overnight in rich medium with 0.2% rhamnose, effectively priming the cells with dCas9. When grown in M9+PA with and without rhamnose, we again observed strong repression of growth (~30-fold) in all conditions regardless of the presence of rhamnose in the M9+PA, and at levels similar to the Δ*paaABCDE* mutant (Figure 2D). This suggests that after the inducer is removed, dCas9 is either slowly degraded in K56-2 or is present at high enough levels in the cells for durable repression.

Single-cell analysis reveals an 'all or none' effect in B. cenocepacia K56-2

While at the culture level the effect of CRISPRi is tunable, we further explored the effect of maximum dCas9 induction at the single-cell level. We therefore targeted *fliF,* a gene encoding a transmembrane protein that forms the M ring of the basal body complex of the flagellum. We targeted *fliF* by introducing four sgRNAs designed to bind near the putative promoter and start codon (Supplemental Figure 5A). Our goal was to assess individual cell flagellation as it compares to overall culture swimming motility, and indeed, insertional inactivation of *fliF* completely ablates swimming motility (Supplemental Figure 5B), supporting previous findings (Tomich et al., 2002). While we observed effective inhibition of swimming motility compared to controls in a plate-based assay (approximately 4-fold reduction) (Supplemental Figure 5B and C), we were

193 unable to observe flagella in any of the mutants harbouring gRNAs targeting *fliF* (Supplemental
194 Figure 5D). It is possible that interfering with *fliF* expression rendered fragile flagella that could
195 not remained attached to the cell during the staining process, while still being functional when
196 grown in culture (Komatsu et al., 2016).

197 As a second option, we targeted *phbC,* a gene encoding poly-β-hydroxybutyrate
198 polymerase, an enzyme required for PHB synthesis. To repress *phbC* expression, we designed
199 three sgRNAs to target the region up to 50 bp before the start codon, at the putative promoter site
200 (Figure 3A). Polyhydroxyalkanoate (PHA) granule accumulation was assessed by fluorescence
201 microscopy with Nile red staining after overnight induction with rhamnose. For comparison to a
202 null phenotype, we created a *phbC* insertional mutant (*phbC*::pAH27) which was unable to
203 produce PHA granules (Figure 3B and D). Compared to the wild-type and non-target controls,
204 markedly few cells harbouring sgRNAs targeting *phbC* contained PHA granules, ranging from 17-
205 70% depending on the sgRNA (Figure 3B). sgRNA6 rendered the strongest level of repression,
206 with only 17.1% of cells containing PHA granules in contrast to 86.9% for the wild-type (Figure
207 3B). Interestingly, although few cells possessed PHA granules, the granules were of identical size
208 to those in wild-type cells, averaging 0.65 μm in diameter (Figure 3C and D). As shown by the
209 insertional mutant, inactivation of *phbC* ablates PHA granule accumulation; therefore, the
210 presence of granules of the same size in the dCas9 mutants as in the wild-type is indicative of an
211 'all-or-none' effect in *B. cenocepacia* K56-2, where most cells display the silenced phenotype, but
212 some manage to escape the effect of CRISPRi.

213 *Broad host range of the mini-CTX system extends applicability to other species*

214 Having shown that the *S. pyogenes* dCas9 renders strong gene repression in *B.* cenocepacia
215 K56-2, we next turned our attention to other important species of *Burkholderia.* We introduced the

codon-optimized *dcas9* gene into the chromosome of *B. multivorans* ATCC 17616 and targeted the *paaA* and *phbC* genes by designing three sgRNAs for each centered around the putative promoter (Figures 4A and C). Targeted repression of *paaA* by each of the three sgRNAs strongly suppressed growth in M9+PA by approximately 25-fold (Figure 4B), very similar to the activity observed in *B. cenocepacia* K56-2. However, we observed poor expression of dCas9 by immunoblot (Supplemental Figure 6A). Given that the observed phenotype is indicative of effective gene silencing, it is unlikely that the actual expression of dCas9 is as low as detected by immunoblot; however, the basis for this discrepancy is unknown. Expression of dCas9 in the presence of the non-targeting sgRNA did not affect growth in *B. multivorans* ATCC 17616 (Supplemental Figure 4C). Following this, targeting *phbC* rendered relatively poor inhibition of PHA granule accumulation with between 35-50% of cells containing PHA granules, depending on the sgRNA (Figure C and D). In contrast to what was seen in *B. cenocepacia* K56-2, we observed granules of reduced size (Figure 4E and F), suggesting there might be compensatory PHA synthesis pathways in *B. multivorans* ATCC 17616.

Members of the *B. pseudomallei* group are phylogenetically distinct from the Bcc (Eberl and Vandamme, 2016), but remain of interest due to the ability to cause infection (such as melioidosis and glanders) and for their remarkable capacity for secondary metabolite production (Mao et al., 2017). *B. thailandensis* is a commonly used model for the pathogenic members of the *B. pseudomallei* group, we therefore also introduced the codon-optimized *dcas9* gene into the chromosome of *B. thailandensis* strain E264. When induced with rhamnose, dCas9 was highly expressed (Supplemental Figure 6) and did not impair growth in the presence of a non-targeting sgRNA (Supplemental Figure 4C). Similarly, as for *B. cenocepacia* K56-2 and *B. multivorans* ATCC 17616, we designed three sgRNAs targeting the putative promoters of the *paaA* and *phbC*

239 genes (Figure 5A and C). Upon induction of dCas9 with 0.2% rhamnose, growth of the mutants
240 harbouring the *paaA*-targeting sgRNAs was suppressed in M9+PA to varying levels ranging from
241 3-fold (sgRNA19) to 25-fold (sgRNA20) (Figure 5B). The fact that some sgRNAs yielded only
242 modest repression was not unexpected as the work characterizing the *paaA* promoter done in K56-
243 2 (Pribytkova et al., 2014) would not likely apply as well to E264 as to the more closely related
244 ATCC 17616. Lastly, for the sgRNAs targeting *phbC*, the results mirror those seen in ATCC
245 17616, as depending on the sgRNA there was variation in the percent of cells with PHA granules
246 (10-40%) and the diameter of the granules (overall decrease in size) (Figure 5C and F). Though
247 the exact contributions to PHA synthesis in E264 remain unclear, it has been previously suggested
248 that PhbC is not the only polyhydroxyalkanoate polymerase in E264 (Funston et al., 2017).

249 The integration vector we implemented to deliver *dcas9* to the chromosome of various
250 species of *Burkholderia* relies on the expression of the φCTX integrase and recombination using
251 the plasmid-borne *attP* site with the chromosomal *attB* site. φCTX is a *Pseudomonas*-infecting
252 phage, and the mini-CTX integration system was originally designed for use in *P. aeruginosa*
253 (Hoang et al., 2000). The mini-CTX integration system has been used successfully in other species;
254 however, this has been mostly limited to members of *Burkholderia* (Chapalain et al., 2017; Le
255 Guillouzer et al., 2017). The utility in *Burkholderia* has been comparable to *P. aeruginosa*, in part
256 owing to efficient integration. In the species used in this study, we observed the integration
257 efficiencies to be $6x10^{-7}$ in K56-2, $6x10^{-8}$ in E264, and $5x10^{-9}$ in ATCC 17616 (Supplemental
258 Figure 7A), compared to 10^{-7} to 10^{-8} observed previously in *P. aeruginosa* (Hoang et al., 2000).
259 To further broaden the scope of the applicability of our CRISPRi system, we used NCBI BLAST
260 to search all published genomes for putative *attB* sites. While the full-length *attB* site is 30 nt,
261 integration is known to occur if only the 5' 19 nt are completely complementary, such as for many

species of *Burkholderia*. This shorter *attB* site was therefore used as a BLAST query, resulting in 1760 hits with 100% alignment (Supplementary Table 4). Enterobacteria were excluded from the search as the pMB1 *oriR* in the mini-CTX system is functional is these species; therefore, integrants cannot be easily isolated. Furthermore, the search parameters were modified to only include species of Proteobacteria. Overall, there were 168 unique species from 67 genera. As expected, the most abundant hit corresponded to species and strains of *Pseudomonas* (480 hits), then followed by *Acinetobacter* (443 hits), *Burkholderia* (276 hits), *Neisseria* (170 hits), and *Ralstonia* (146 hits), with members of the other 62 genera comprising the remaining 245 hits. A summary of the major hits and species of interest (pathogenic, environmental, biotechnological, etc) can be found along with the genomic context in Table 1. We note that the hit table comprises species with both high and low GC-content genomes, and while the GC-rich codon-optimized *dcas9* (in pAH-CTX1-rhadCas9) may be better suited for species with high GC-content genomes, such as those in the families *Pseudomonadaceae* and *Alcaligenaceae*, the native *dcas9* (in pAH-CTX1-rhadCas9-native) may have better functionality in species with low GC-content genomes, such as those in the families *Moraxellaceae* and *Neisseriaceae*.

A further consideration for use of our CRISPRi system is that the pFLPe recombinase-expressing plasmids might not be functional in all species. In which case, the *int* and *tet* genes along with the *oriT* and pBM1 *oriR* would not be excised and the mutant would remain resistant to tetracycline. To explore if experiments could be performed in the absence of tetracycline selection, we assessed the stability of the mini-CTX integration in K56-2, ATCC 17616, and E264 in serial passages over four days without tetracycline. For all species over the entire experiment we determined CFU counts on agar with and without tetracycline selection and found equal

284 recovery of tetracycline-resistant colonies as total colonies (Supplemental Figure 7B-D),
285 suggesting the integration is stable.

286

287 **Discussion**

288 Genetic tools are necessary to dissect the molecular mechanisms governing cellular
289 processes. Here, we report the development of a CRISPRi system for efficient repression of gene
290 expression in *Burkholderia*. By mobilizing the *dcas9* gene that was codon-optimized for the GC-
291 rich *Burkholderia* on a broad host range mini-CTX1 integration vector, we demonstrate robust,
292 tunable, and durable repression of endogenous genes. While others have shown effective
293 repression using the native *dcas9* gene in *E. coli* (Qi et al., 2013), *B. subtilis* (Peters et al., 2016),
294 *Staphylococcus aureus*, and *Acinetobacter baumannii* (Peters et al., 2019), codon-optimization
295 was a necessary step for K56-2, as expression of the native *dcas9* gene was not detectable in K56-
296 2. Indeed, for expression in species with high GC-content, codon optimization appears to be
297 necessary. In *P. aeruginosa* (66.3% GC) both the *S. pyogenes* dCas9 (Peters et al., 2019) and the
298 *S. pasteurianus* dCas9 (Tan et al., 2018) were not expressed unless first codon-optimized, albeit
299 for *Mycobacterium* (~67% GC) or *Homo sapiens* (optimized at 50.2% GC). Additionally, the *S.*
300 *thermophilus* dCas9 was codon-optimized for *Mycobacterium* for efficient expression in *M.*
301 *tuberculosis* and *M. smegmatis* (Rock et al., 2017).

302 Despite codon-optimizing the *dcas9* gene, we observe a severe growth defect when
303 expressed from a multicopy pBBR1 origin plasmid. At this time, we are unsure if this was caused
304 by a metabolic burden of expressing a large protein from a multicopy plasmid or from direct
305 proteotoxicity. Previous studies have demonstrated that expression of the canonical *S. pyogenes*

dCas9 causes toxicity in *M. smegmatis*, *M. tuberculosis* (Rock et al., 2017), and *E. coli* (Cho et al., 2018), which provides rationale for developing a system with low-enough levels of dCas9 expression to maintain cell viability without sacrificing repression activity. While this effort has spurred the exploration of alternative dCas9 orthologues (Rock et al., 2017), we found that introducing *dcas9* in single copy in the chromosome provided a balance of repression activity without affecting growth. Furthermore, while other systems display up to 3-fold repression in the absence of inducer (Peters et al., 2016; Tan et al., 2018), our application of the tightly regulated rhamnose-inducible promoter from *E. coli* does not display such a phenomenon in any of the three species tested. Consequently, we suggest this attribute is suited for the investigation of essential genes, as we would predict wild-type growth in the absence of inducer. However, at the cost of apparently negligible uninduced expression, the rhamnose-inducible promoter is incapable of attaining the high levels of maximal expression seen in other systems, such as the xylose-inducible promoter used in the *B. subtilis* CRISPRi library (Peters et al., 2016) (Supplementary Figure 4A). While we did observe increased expression at rhamnose concentrations of 0.5% and 1.0%, it was accompanied by a substantial growth defect. This is similar to the use of the arabinose-inducible promoter in K56-2, in which the 2-3% arabinose necessary to induce maximal expression caused marked changes in cell morphology reminiscent of osmotic stress (Cardona and Valvano, 2005). As a result of the lower levels of maximal expression, it remains possible that our CRISPRi system may not be capable of effectively repressing highly transcribed genes, but this is under investigation. While work by Vigouroux et al. (Vigouroux et al., 2018) suggests that when the sgRNA binding site is saturated with the dCas9:sgRNA complex, fold change in repression is independent of promoter strength; however, the absolute repression of highly active promoters is lower and it is unclear what constitutes saturating levels of dCas9. Furthermore, multiplexing

CRISPRi with simultaneous use of more than one sgRNA might reduce the repression at each locus by titrating away dCas9, and this effect may be even more apparent if lower levels of dCas9 are present.

Critical to fine manipulation of gene expression in precision experiments is tunability. We show that using the rhamnose-inducible promoter can provide intermediate levels of repression and a resulting phenotype of gene depletion rather than complete silencing. Combined with the lack of repression in the uninduced state, we propose that our CRISPRi system will be useful in providing dynamic gene repression. Moreover, the repression caused by dCas9 is durable, as even a full 24 hours after removal of the inducer, we observed the same phenotype as in the cultures grown with inducer. This is in line with previous findings in *Giardia lamblia* (McInally et al., 2019) and *in vitro* (Jones et al., 2017; Sternberg et al., 2014). Interestingly, binding of the dCas9:sgRNA complex to a target is nearly irreversible once the sgRNA has bound with complete complementarity to its target site (Sternberg et al., 2014). Furthermore, this means that the dCas9:sgRNA complex does not follow Michaelis-Menton enzyme kinetics, with each dCas9 acting like a single-turnover enzyme that, *in vitro*, can only be removed from the target by strong detergents (Sternberg et al., 2014). *In vivo* however, although the RNA polymerase is largely incapable of displacing the dCas9:sgRNA complex, the DNA replication machinery is not blocked by dCas9. In fact, it has been observed that the dissociation of the dCas9:sgRNA complex correlates well with the generation time in *E. coli* (Jones et al., 2017). This is an important consideration for understanding the durability of growth suppression we observed when using PA as a sole carbon source. When priming the cells by pre-incubation with rhamnose and then placing the cells in M9+PA, they were unable to grow, that is *paaA* became a conditionally essential gene, thereby shutting down cell division and DNA replication. Hence, the DNA replication machinery

would not displace the dCas9:sgRNA from the *paaA* gene, resulting in long-term growth suppression. By extension, we predict that strong knockdown of any (conditionally) essential gene that causes a halt in DNA replication would be durable in this manner. This is a useful aspect of CRISPRi that we are investigating further.

Although it has been reported that the CRISPRi system is less effective in silencing the gene expression when the template strand (T) is targeted compared to the non-template (NT) strand, our results demonstrated nearly 30-fold repression of the growth irrespective of the *paaA* target strand (Figure 2B). This suggests that the efficiency of the CRISPRi system might not strand specific at all loci, supporting the findings from Howe et al. (Howe et al., 2017). However, this effect might have been masked by the strong repression we observed, as it is difficult to compare across null phenotypes. Additionally, sgRNAs targeting different regions of the 5' region of *paaA* produced a strong 25-30-fold repression in all three species studied here, suggesting that knockdown efficiency is largely unaffected by sgRNA placement on targeting regions overlapping or adjacent to the −35 and −10 promoter elements. possibly resulted from the proximity of the large dCas9:sgRNA complex to the promoter sterically interfering with the RNA polymerase binding. Indeed, the ~160 kDa dCas9 enzyme has an average DNA footprint of 78.1 bp, much larger than most promoter regions (Josephs et al., 2015).

Single cell level analysis of our system demonstrated a unimodal 'all or none' effect in K56-2 with ~17% cells escaping the silenced phenotype when targeting *phbC* compared to an insertion mutant, which did not possess any granules. The PHB granules in these cells were of identical diameter to wild type, averaging 0.65µm in diameter. The 'all or none' effect might be attributed to an uneven distribution of the membrane transporter involved in transporting rhamnose into the cell, essentially escaping the rhamnose mediated *dCas9* induction to silence the target gene

(Siegele and Hu, 1997). Interestingly, targeting *phbC* in *B. multivorans* ATCC17616 and *B. thailandensis* E264 resulted in a mixed phenotype with a reduced number of cells with granules as well as an overall decrease in granule size. Even though some of the cells seemed to have escaped the repression (up to 35% in ATCC17616 and 6% in E264), more than 90% of the cells contained granules of reduced size. The residual presence of PHA granule suggests the existence of an unelucidated PHA synthesis pathways in *B. thailandensis* E264 and *B. multivorans* ATCC 17616, supporting the finding from Funston et al. (Funston et al., 2017).

One of the hallmarks of CRISPRi is the broad-range amenability in diverse bacteria, enabling synthetic biology and mechanistic investigations into many dozens of species in innovative ways. We wished to apply our CRISPRi system in this manner and therefore mobilized both the native *dcas9* gene, suitable for low/medium GC-content organisms, and the *dcas9* gene, codon-optimized for GC-rich *Burkholderia*, on the mini-CTX1 integration vector. Our analysis of putative hosts (with *attB* sites near the 3' end of the serine tRNA) identified 168 unique species in 67 genera, mostly from the β- and γ-Proteobacteria. Previous works have mobilized *dcas9* on broad host-range integrative plasmids (Peters et al., 2019; Tan et al., 2018); however, both systems use the mini-*Tn*7 system, which has multiple insertion locations in certain genomes, such as many species of *Burkholderia*. Together, our work contributes to the available genetic toolkit for rapid functional analysis of bacteria.

Methods

Strains, selective antibiotics, and growth conditions

All strains and plasmids are found in Supplemental Table 1. All strains were grown in LB-Lennox medium (Difco). *B. cenocepacia* K56-2 and strains of *E. coli* were grown at 37°C, while

B. thailandensis E264 and *B. multivorans* ATCC 17616 were grown at 30°C. The following selective antibiotics were used: chloramphenicol (Sigma; 100 μg/mL for *B. cenocepacia,* 20 μg/mL for *E. coli*), trimethoprim (Sigma; 100 μg/mL for strains of *Burkholderia*, 50 μg/mL for *E. coli*), tetracycline (Sigma; 50 μg/mL for all strains of *Burkholderia*, 20 μg/mL for *E. coli*), kanamycin (250 μg/mL for *B. thailandensis*, 150 μg/mL for *B. multivorans*, 40 μg/mL for *E. coli*), ampicillin (100 μg/mL for *E. coli*), gentamicin (50 μg/mL for all strains of *Burkholderia*).

Construction of pSC-rhadCas9, pAH-CTX1-rhadCas9, pAH-CTX1-rhadCas9-native, and dCas9 insertional mutants

The endogenous *cas9* gene from *S. pyogenes* has low GC content (averaging 34.1%) and subsequently poor codon usage for GC-rich organisms (http://www.kazusa.or.jp/codon/). The nuclease-inactive variant (*dcas9*) was therefore codon optimized for *B. cenocepacia* by purchasing the optimized gene in two fragments from IDT (2462 bp and 1849 bp, Supplemental table 2), each with 38 bp overlapping regions. Strong, rho-independent terminators were added following the gene. The full-length gene (with terminal *Nde*I and *Hind*III cut sites) was synthesized by overlap-extension PCR using Q5 polymerase with high GC buffer (NEB) and primers 979 and 987 (Supplemental Table 2). The first ten rounds of PCR were performed without primers to synthesize the full-length product using the overlap regions; primers were added for the following 25 cycles. The cycle parameters are as follows: 98°C for 30 sec, (98°C for 10 sec, 67.5°C for 20 sec, 72°C for 2.5 min)x10 cycles, 72°C for 5 min, 98°C for 30 sec, (98°C for 10 sec, 62.5°C for 20 sec,72 °C for 2.5 min)x25 cycles, 72°C for 10 min. The 4267 bp product was gel-purified (Qiagen) and introduced into pSCrhaB2 by restriction cloning using *Nde*I and *Hind*III (NEB). The resulting plasmid, pSC-rhadCas9, was transformed into *E. coli* DH5α, and trimethoprim-resistant colonies

were screened by colony PCR with primers 954 and 955. Triparental mating with *E.* coli MM290/pRK2013 as a helper was performed as previously described (Hogan et al., 2018).

Serial restriction cloning was used to introduce the optimized *dcas9* into the mini-CTX1 insertion plasmid (Hoang et al., 2000). The rhamnose-inducible promoter from pSC201 (Ortega et al., 2007) was first PCR amplified with Q5 polymerase and primers 976 and 1071, containing *Hind*III and *Spe*I restriction sites, respectively. This fragment was introduced into mini-CTX1, to create pAH-CTX1-rha, and tetracycline-resistant *E. coli* DH5α were screened by colony PCR using primers 957 and 1074. The fragment containing the dCas9 gene was PCR amplified as above, but instead using primers 1072 and 1073, introducing *Spe*I and *Not*I restriction sites, respectively. This fragment was introduced into pAH-CTX1-rha, to create pAH-CTX1-rhadCas9, and tetracycline-resistant *E. coli* DH5α colonies were screened by colony PCR using primers 954 and 955.

The native (non codon-optimized) *dcas9* was also introduced into pAH-CTX1-rha. The native *dcas9* and transcriptional terminators were PCR amplified from pdCas9-bacteria (Addgene plasmid # 44249) with Q5 polymerase (NEB) using primers 1216 and 1217. The PCR product was cloned into pAH-CTX1-rha (creating pAH-CTX1-rhadcas9-native) using *Not*I and *Spe*I restriction sites then transformed into *E. coli* DH5α. Tetracycline-resistant colonies were screened by PCR using primers 954 and 1218.

pAH-CTX1-rha, pAH-CTX1-rhadCas9, and pAH-CTX1-rhadCas9-native were introduced into *Burkholderia* species by triparental mating using *E. coli* MM290/pRK2013 as a helper as above. Tetracycline-resistant colonies were screened by colony PCR using primer 954 (for pAH-CTX1-rha) or 1075 (for pAH-CTX1-rhadCas9) or 1219 (for pAH-CTX1-rhadcas9-native) and 1008 (for *B. cenocepacia*), 1167 (for *B. multivorans*), or 1168 (for *B. thailandensis*).

While the pFLPe plasmids have been used to remove the tetracycline resistance and integrase genes in other species (Choi et al., 2008), sensitive colonies could not be obtained in *B. cenocepacia*. Therefore, the clean deletion method of Flannagan et al was used as previously described (Flannagan et al., 2008). To do this, a fragment with 475 bp overlapping the upstream and downstream regions of the *FRT* sites when pAH-CTX1-rhadCas9 was inserted into the genome (Supplemental Figure 2), was designed and synthesized (IDT) with *Kpn*I and *Eco*RI restriction sites, respectively. The fragment was ligated into pGPI-*Sce*I (Flannagan et al., 2008) via the *Kpn*I and *Eco*RI restriction sites, creating pAH18, and transformed into *E. coli* SY327. Trimethoprim-resistant colonies were screened for the insertion of the fragment with primer 153 and 154. pAH18 was introduced into the mutant backgrounds via triparental mating, as described above. Trimethoprim-resistant K56-2 were screened by PCR for both possible integration orientations using primers 154 and 1126, or 153 and 1133. To initiate the second recombination, an *Sce*I-expressing plasmid is required; however, the conventional plasmid, pDAI-*Sce*I, confers tetracycline resistance and could not be selected for in the mutant background. Therefore, the tetracycline resistance cassette was removed by digestion with *Age*I and *Xho*I. The chloramphenicol resistance gene *cat* was PCR amplified from pKD3 (Datsenko and Wanner, 2000) using primers 1084 and 1150, then ligated into the pDAI-*Sce*I backbone and transformed into *E. coli* DH5α, creating pAH25-*Sce*I. Chloramphenicol-resistant colonies were screened with primers 1091 and 1150. pAH35-*Sce*I was introduced into the mutant backgrounds by triparental mating as described above. Chloramphenicol-resistant colonies were screened for sensitivity to trimethoprim (indicating excision of pAH18) and tetracycline (indicating excision of the genes between the *FRT* sites), and then screened by PCR with primers 1126 and 1133, which bridge the excision.

464 The pFLPe system was used to remove the tetracycline resistance and integrase genes in
465 the dCas9 mutants in *B. multivorans* ATCC 17616 and *B. thailandensis* E264. Triparental mating
466 to introduce pFLPe4 into the strains was performed as for K56-2 above, except 0.2% rhamnose
467 was added to the mating and antibiotic selection plates. Tetracycline-sensitive colonies were
468 screened by PCR using primers 957 and 1194 (for *B. multivorans*) or 1195 (for *B. thailandensis*).
469 pFLPe4 has a temperature-sensitive origin of replication; therefore, mutants were grown overnight
470 in LB without antibiotics at 37^{o}C. Single colonies were then tested for kanamycin sensitivity and
471 then by colony PCR for pFLPe4 using primers 1128 and 1129.

472 *Design and construction of the sgRNA-expressing plasmids*

473 PAM sequences closest to the 5' end of the transcription start site (TSS) were first
474 identified on both the non-template and template strands. We extracted 20-23 nucleotides adjacent
475 to the PAM sequence to design the base-pairing region of the sgRNAs in the following format: 5'-
476 CCN-$N_{(20-23)}$-3' for targeting the non-template strand and 5'$N_{(20-23)}$-NGG-3' for the template
477 strand. To score the specificity and identify off-target binding sites, the 5' end of the 20-23nt
478 variable base-pairing sequences were trimmed one base at a time and the remaining base-pairing
479 region was searched against the appropriate organism's reference genome. This was repeated until
480 only 10 nt was used as a search query. Potential sgRNAs were discarded if off-target sites were
481 discovered in this manner.

482 The expression vector pSCrhaB2 (Cardona and Valvano, 2005) was chosen as the method
483 of sgRNA expression due to the broad host range of the pBBR1 origin of replication. The sgRNA
484 cassette from pgRNA-bacteria (Qi et al., 2013) (Addgene plasmid # 44251) was introduced into
485 pSCrhaB2 by restriction cloning with *Eco*RI and *Hind*III (NEB) to create pSCrhaB2-sgRNA. To
486 remove *rhaS* and *rhaR*, inverse PCR was performed using Q5 polymerase (NEB) and primers 847

and 1025. The resulting fragment was ligated by blunt-end ligation using 1µL of PCR product incubated with 0.5 µL *Dpn*I, 0.5 µL T4 polynucleotide kinase, and 0.5 µL T4 ligase (NEB) with quick ligation buffer (NEB) at 37^{o}C for 30 minutes. The resulting plasmid, pSCB2-sgRNA, was screened using primers 781 and 848, which span the ligated junction. Individual sgRNAs were introduced into pSCB2-sgRNA using inverse PCR as previously described (Qi et al., 2013) (Supplemental Table 3).

Construction of the fliF insertional mutant

Inactivation of *fliF* was performed with the mutagenesis system of Flannagan et al. (Flannagan et al., 2007). Briefly, a 322 bp internal fragment of *fliF* was PCR amplified from the K56-2 genome using primers 1156 and 1157 and Q5 polymerase (NEB). The fragment and pGPΩ-Tp were double digested with *Kpn*I and *Eco*RI (NEB) and ligated with T4 ligase (NEB). The resulting plasmid, pAH26, was electroporated into *E. coli* SY327, and trimethoprim-resistant colonies were screened by colony PCR for the *fliF* fragment. Triparental matings were performed as above. Trimethoprim-resistant exconjugants, were screened by motility assay (below).

Construction of the phbC insertional mutant

Inactivation of *phbC* (WQ49_RS30385) was performed as for *fliF*. Briefly, a 328 bp internal fragment of *phbC* was PCR amplified from the K56-2 genome using primers 1196 and 1197 and Q5 polymerase (NEB). The plasmid, pAH27, created from ligating the fragment into pGPΩ-Tp using *Kpn*I and *Eco*RI (NEB) restriction sites, was electroporated into *E. coli* SY327 and trimethoprim-resistant colonies were screened by colony PCR for the *phbC* fragment. Triparental matings were performed as above, and trimethoprim-resistant exconjugants were screened by staining for polyhydroxyalkanoate granule accumulation (below).

509 *Assays for integration efficiency and stability of the mini-CTX1-based system*

510 To assess integration efficiency, triparental matings were started as above. However, after
511 the mating on LB agar, the pellicles were serially diluted and plated for CFU/mL on LB agar with
512 50 μg/mL gentamicin and LB agar with 50 μg/mL tetracycline and 50 μg/mL gentamicin.

513 To assess stability of the integration, cultures of the dCas9 mutants (containing the
514 tetracycline resistance cassette) were serial passaged over 4 days without antibiotics. Each day, a
515 fresh culture was started by 1:2500 dilution of the previous day's stationary phase culture. In
516 addition, the cultures were serially diluted and plated for CFU/mL on LB agar without antibiotics
517 and LB agar with 50 μg/mL tetracycline.

518 *Growth assay with phenylacetic acid as the sole carbon source*

519 Overnight cultures, started from isolated colonies, of the appropriate strains were washed
520 at 4000x g for 4 minutes and resuspended in PBS (2.7 mM KCl, 136.9 mM NaCl, 1.5 mM KH_2PO_4,
521 8.9 mM Na_2HPO_4, pH 7.4) to remove growth medium. The OD_{600nm} of the cultures was normalized
522 to 0.01 in M9 medium supplemented with 5 mM phenylacetic acid, 100 μg/mL trimethoprim, and
523 0.2% rhamnose as required. The culture was added to wells of a 96-well plate and incubated with
524 continuous shaking at 37°C (for *B. cenocepacia* K56-2) or 30°C (for *B. multivorans* ATCC 17616
525 and *B. thailandensis* E264). The OD_{600nm} of the cultures was measured after 24 hours for *B.*
526 *cenocepacia* K56-2 and *B. multivorans* ATCC 17616, or 48 hours for *B. thailandensis* E264.

527 *Fluorescent microscopy and polyhydroxyalkanoate granule detection*

528 Overnight cultures of the appropriate strains with or without rhamnose were first washed
529 to remove growth medium and resuspended in PBS. Cells were fixed in 3.7% formaldehyde + 1%
530 methanol at room temperature for 10 minutes (*B. cenocepacia* K56-2) or 20 minutes (*B.*

multivorans ATCC 17616 and *B. thailandensis* E264) then quenched by the addition of an equal volume of 0.5 M glycine. The cells were washed and resuspended in PBS with 0.5 μg/mL Nile Red (Carbosynth) and stained at room temperature in the dark for 20 minutes, after which the cells were washed to remove excess stain and resuspended in PBS. The cells were mounted on 1.5% agarose pads and imaged by fluorescence microscopy at 1000x total magnification on an upright AxioImager Z1 (Zeiss). Nile red was excited at 546/12 nm and detected at 607/33 nm.

Plate-based motility assay

Assays were performed as previously described (Kumar and Cardona, 2016), with some modifications. Briefly, strains were grown on LB agar with the appropriate antibiotics and single colonies were stab-inoculated into motility medium consisting of nutrient broth (Difco) with 0.3% agar. Medium was supplemented with rhamnose (Sigma) as appropriate. Plates were incubated right-side up for 22 hours at 37^{o}C.

Flagellum staining

Staining was performed as previously described (Kumar and Cardona, 2016). Briefly, an overnight culture was rested statically at room temperature for 20 minutes. Gently, a 1 in 10 dilution was prepared in water and rested statically for a further 20 minutes. A small drop of the diluted culture was placed on a clean glass slide and rested for 20 minutes. A coverglass was gently applied and one side was flooded with Ryu flagellum stain (Remel), then allowed to dry for 2 hours at room temperature. Slides were observed by light microscopy at 1000x total magnification on an upright AxioImager Z1 (Zeiss).

553 *SDS-PAGE and Immunoblotting*

554 Cells from an overnight culture were subcultured into fresh medium and grown at 37°C
555 (30°C for *B. thailandensis*) to an OD_{600nm} of 0.4, then exposed to various concentrations of
556 rhamnose for 3 hours. Soluble protein was isolated first by sonicating the cells in TNG Buffer (100
557 mM Tris-HCl, 150 mM NaCl, 10% glycerol, pH 7.4) then by centrifugation at 15 000g for 20
558 minutes. Following boiling denaturation in SDS loading buffer (50 mM Tris-HCl, 2% SDS, 0.2%
559 bromophenol blue, 20% glycerol, 100 mM DTT, pH 6.8), samples were run on an 8% Tris/glycine
560 gel. To ensure equal loading, 20 µg protein was loaded per well (as determined by NanoDrop) and
561 gels were run in duplicate (one for immunoblot, and another for Coomassie staining). Protein was
562 transferred by iBlot to a PVDF membrane, blocked in 5% skim milk-TBST (150 mM NaCl, 10
563 mM Tris-HCl, 0.5% Tween-20, pH 7.5) at room temperature for 1 hour, then probed with a 1:2
564 000 dilution of primary α-Cas9 antibody (ThermoFisher 10C11-A12) in 5% skim milk-TBST
565 overnight at 4°C. Following washes, the blot was probed with a 1:20 000 dilution of secondary
566 antibody linked to alkaline phosphatase (ThermoFisher G-21060) in 5% skim milk-TBST for 1
567 hour at room temperature. Protein was detected by incubation with a solution of NBT/BCIP
568 (Roche) as per the manufacturer's protocols.

569

Acknowledgements

This work was financially supported by grants from the Cystic Fibrosis Foundation, Cystic Fibrosis Canada, and the Natural Sciences and Engineering Research Council of Canada (NSERC) to STC; AMH was supported by grants from the Canadian Institutes of Health Research (CIHR) and Cystic Fibrosis Canada.

The authors are grateful to Eric Déziel from the Institut National de la Recherche Scientifique – Institut Armand-Frappier for providing the miniCTX1 integration vector.

Conflict of Interest Statement

The authors declare no conflict of interest.

References

Bikard, D., Jiang, W., Samai, P., Hochschild, A., Zhang, F., and Marraffini, L.A. (2013). Programmable repression and activation of bacterial gene expression using an engineered CRISPR-Cas system. Nucleic Acids Res. *41*, 7429–7437.

Cardona, S.T., and Valvano, M.A. (2005). An expression vector containing a rhamnose-inducible promoter provides tightly regulated gene expression in *Burkholderia cenocepacia*. Plasmid *54*, 219–228.

Chapalain, A., Groleau, M.-C., Le Guillouzer, S., Miomandre, A., Vial, L., Milot, S., and Déziel, E. (2017). Interplay between 4-Hydroxy-3-Methyl-2-Alkylquinoline and N-Acyl-Homoserine Lactone Signaling in a Burkholderia cepacia Complex Clinical Strain. Front. Microbiol. *8*, 1021.

591 Cho, S., Choe, D., Lee, E., Kim, S.C., Palsson, B., and Cho, B.-K. (2018). High-Level dCas9
592 Expression Induces Abnormal Cell Morphology in Escherichia coli. ACS Synth. Biol.

593 Cho, S.W., Kim, S., Kim, J.M., and Kim, J.-S. (2013). Targeted genome engineering in human
594 cells with the Cas9 RNA-guided endonuclease. Nat. Biotechnol. *31*, 230–232.

595 Choi, K.-H., and Schweizer, H.P. (2006). mini-Tn7 insertion in bacteria with single attTn7 sites:
596 example Pseudomonas aeruginosa. Nat. Protoc. *1*, 153–161.

597 Choi, K.H., Gaynor, J.B., White, K.G., Lopez, C., Bosio, C.M., Karkhoff-Schweizer, R.R., and
598 Schweizer, H.P. (2005). A Tn7-based broad-range bacterial cloning and expression system.
599 Nat.Methods *2*, 443–448.

600 Choi, K.H., DeShazer, D., and Schweizer, H.P. (2006). mini-Tn7 insertion in bacteria with
601 multiple glmS-linked attTn7 sites: example *Burkholderia mallei* ATCC 23344. Nat. Protoc. *1*,
602 162–169.

603 Choi, K.H., Mima, T., Casart, Y., Rholl, D., Kumar, A., Beacham, I.R., and Schweizer, H.P.
604 (2008). Genetic tools for select-agent-compliant manipulation of *Burkholderia pseudomallei*.
605 Appl. Environ. Microbiol. *74*, 1064–1075.

606 Choudhary, E., Thakur, P., Pareek, M., and Agarwal, N. (2015). Gene silencing by CRISPR
607 interference in mycobacteria. Nat. Commun. *6*, ncomms7267.

608 Cui, L., Vigouroux, A., Rousset, F., Varet, H., Khanna, V., and Bikard, D. (2018). A CRISPRi
609 screen in E. coli reveals sequence-specific toxicity of dCas9. Nat. Commun. *9*, 1912.

610 Darling, P., Chan, M., Cox, A.D., and Sokol, P.A. (1998). Siderophore production by cystic
611 fibrosis isolates of *Burkholderia cepacia*. Infect. Immun. *66*, 874–877.

612 Datsenko, K.A., and Wanner, B.L. (2000). One-step inactivation of chromosomal genes in
613 *Escherichia coli* K-12 using PCR products. Proc Natl Acad Sci U A *97*, 6640–6645.

614 Depoorter, E., Bull, M.J., Peeters, C., Coenye, T., Vandamme, P., and Mahenthiralingam, E.
615 (2016). Burkholderia: an update on taxonomy and biotechnological potential as antibiotic
616 producers. Appl. Microbiol. Biotechnol. *100*, 5215–5229.

617 Eberl, L., and Vandamme, P. (2016). Members of the genus *Burkholderia*: good and bad guys.
618 F1000Research *5*, 1007.

619 Figurski, D.H., and Helinski, D.R. (1979). Replication of an origin-containing derivative of
620 plasmid RK2 dependent on a plasmid function provided in trans. Proc. Natl. Acad. Sci. U. S. A.
621 *76*, 1648–1652.

622 Flannagan, R.S., Aubert, D., Kooi, C., Sokol, P.A., and Valvano, M.A. (2007). Burkholderia
623 cenocepacia requires a periplasmic HtrA protease for growth under thermal and osmotic stress and
624 for survival *in vivo*. Infect. Immun. *75*, 1679–1689.

625 Flannagan, R.S., Linn, T., and Valvano, M.A. (2008). A system for the construction of targeted
626 unmarked gene deletions in the genus *Burkholderia*. Environ. Microbiol. *10*, 1652–1660.

627 Funston, S.J., Tsaousi, K., Smyth, T.J., Twigg, M.S., Marchant, R., and Banat, I.M. (2017).
628 Enhanced rhamnolipid production in Burkholderia thailandensis transposon knockout strains
629 deficient in polyhydroxyalkanoate (PHA) synthesis. Appl. Microbiol. Biotechnol. *101*, 8443–
630 8454.

631 Hoang, T.T., Kutchma, A.J., Becher, A., and Schweizer, H.P. (2000). Integration-proficient
632 plasmids for Pseudomonas aeruginosa: site-specific integration and use for engineering of reporter
633 and expression strains. Plasmid *43*, 59–72.

634 Hogan, A.M., Scoffone, V.C., Makarov, V., Gislason, A.S., Tesfu, H., Stietz, M.S., Brassinga,
635 A.K.C., Domaratzki, M., Li, X., Azzalin, A., et al. (2018). Competitive Fitness of Essential Gene
636 Knockdowns Reveals a Broad-Spectrum Antibacterial Inhibitor of the Cell Division Protein FtsZ.
637 Antimicrob. Agents Chemother. *62*.

638 Howe, C., Sampath, A., and Spotnitz, M. (1971). The pseudomallei group: a review. J. Infect. Dis.
639 *124*, 598–606.

Howe, F.S., Russell, A., Lamstaes, A.R., El-Sagheer, A., Nair, A., Brown, T., and Mellor, J. (2017). CRISPRi is not strand-specific at all loci and redefines the transcriptional landscape. ELife *6*.

Jones, D.L., Leroy, P., Unoson, C., Fange, D., Ćurić, V., Lawson, M.J., and Elf, J. (2017). Kinetics of dCas9 target search in Escherichia coli. Science *357*, 1420–1424.

Josephs, E.A., Kocak, D.D., Fitzgibbon, C.J., McMenemy, J., Gersbach, C.A., and Marszalek, P.E. (2015). Structure and specificity of the RNA-guided endonuclease Cas9 during DNA interrogation, target binding and cleavage. Nucleic Acids Res. *43*, 8924–8941.

Judson, N., and Mekalanos, J.J. (2000). TnAraOut, a transposon-based approach to identify and characterize essential bacterial genes. Nat Biotechnol *18*, 740–745.

Kenna, D.T.D., Lilley, D., Coward, A., Martin, K., Perry, C., Pike, R., Hill, R., and Turton, J.F. (2017). Prevalence of Burkholderia species, including members of Burkholderia cepacia complex, among UK cystic and non-cystic fibrosis patients. J. Med. Microbiol. *66*, 490–501.

Komatsu, H., Hayashi, F., Sasa, M., Shikata, K., Yamaguchi, S., Namba, K., and Oosawa, K. (2016). Genetic analysis of revertants isolated from the rod-fragile fliF mutant of Salmonella. Biophys. Physicobiology *13*, 13–25.

Kumar, B., and Cardona, S.T. (2016). Synthetic Cystic Fibrosis Sputum Medium Regulates Flagellar Biosynthesis through the flhF Gene in *Burkholderia* cenocepacia. Front. Cell. Infect. Microbiol. *6*, 65.

Le Guillouzer, S., Groleau, M.-C., and Déziel, E. (2017). The Complex Quorum Sensing Circuitry of Burkholderia thailandensis Is Both Hierarchically and Homeostatically Organized. MBio *8*.

Lee, H.H., Ostrov, N., Wong, B.G., Gold, M.A., Khalil, A.S., and Church, G.M. (2019). Functional genomics of the rapidly replicating bacterium Vibrio natriegens by CRISPRi. Nat. Microbiol.

Liu, X., Gallay, C., Kjos, M., Domenech, A., Slager, J., van Kessel, S.P., Knoops, K., Sorg, R.A., Zhang, J.-R., and Veening, J.-W. (2017). High-throughput CRISPRi phenotyping identifies new essential genes in Streptococcus pneumoniae. Mol. Syst. Biol. *13*, 931.

Mahenthiralingam, E., Urban, T.A., and Goldberg, J.B. (2005). The multifarious, multireplicon *Burkholderia cepacia* complex. Nat. Rev. Microbiol. *3*, 144–156.

Mao, D., Bushin, L.B., Moon, K., Wu, Y., and Seyedsayamdost, M.R. (2017). Discovery of scmR as a global regulator of secondary metabolism and virulence in *Burkholderia thailandensis* E264. Proc. Natl. Acad. Sci. U. S. A. *114*, E2920–E2928.

McInally, S.G., Hagen, K.D., Nosala, C., Williams, J., Nguyen, K., Booker, J., Jones, K., and Dawson, S.C. (2019). Robust and stable transcriptional repression in Giardia using CRISPRi. Mol. Biol. Cell *30*, 119–130.

Miller, V.L., and Mekalanos, J.J. (1988). A novel suicide vector and its use in construction of insertion mutations: osmoregulation of outer membrane proteins and virulence determinants in *Vibrio cholerae* requires *toxR*. J. Bacteriol. *170*, 2575–2583.

Nally, E., Groah, S.L., Pérez-Losada, M., Caldovic, L., Ljungberg, I., Chandel, N.J., Sprague, B., Hsieh, M.H., and Pohl, H.G. (2018). Identification of Burkholderia fungorum in the urine of an individual with spinal cord injury and augmentation cystoplasty using 16S sequencing: copathogen or innocent bystander? Spinal Cord Ser. Cases *4*, 85.

Ortega, X.P., Cardona, S.T., Brown, A.R., Loutet, S.A., Flannagan, R.S., Campopiano, D.J., Govan, J.R., and Valvano, M.A. (2007). A putative gene cluster for aminoarabinose biosynthesis is essential for *Burkholderia cenocepacia* viability. J. Bacteriol. *189*, 3639–3644.

Peters, J.M., Colavin, A., Shi, H., Czarny, T.L., Larson, M.H., Wong, S., Hawkins, J.S., Lu, C.H., Koo, B.M., Marta, E., et al. (2016). A comprehensive, CRISPR-based functional analysis of essential genes in bacteria. Cell *165*, 1493–1506.

Peters, J.M., Koo, B.-M., Patino, R., Heussler, G.E., Hearne, C.C., Qu, J., Inclan, Y.F., Hawkins, J.S., Lu, C.H.S., Silvis, M.R., et al. (2019). Enabling genetic analysis of diverse bacteria with Mobile-CRISPRi. Nat. Microbiol. *4*, 244.

Pribytkova, T., Lightly, T.J., Kumar, B., Bernier, S.P., Sorensen, J.L., Surette, M.G., and Cardona, S.T. (2014). The attenuated virulence of a Burkholderia cenocepacia paaABCDE mutant is due to inhibition of quorum sensing by release of phenylacetic acid. Mol. Microbiol. *94*, 522–536.

693 Qi, L.S., Larson, M.H., Gilbert, L.A., Doudna, J.A., Weissman, J.S., Arkin, A.P., and Lim, W.A.
694 (2013). Repurposing CRISPR as an RNA-guided platform for sequence-specific control of gene
695 expression. Cell *152*, 1173–1183.

696 Rhodes, K.A., and Schweizer, H.P. (2016). Antibiotic resistance in Burkholderia species. Drug
697 Resist. Updat. *28*, 82–90.

698 Rock, J.M., Hopkins, F.F., Chavez, A., Diallo, M., Chase, M.R., Gerrick, E.R., Pritchard, J.R.,
699 Church, G.M., Rubin, E.J., Sassetti, C.M., et al. (2017). Programmable transcriptional repression
700 in mycobacteria using an orthogonal CRISPR interference platform. Nat. Microbiol. *2*, 16274.

701 Siegele, D.A., and Hu, J.C. (1997). Gene expression from plasmids containing the araBAD
702 promoter at subsaturating inducer concentrations represents mixed populations. Proc Natl Acad
703 Sci U A *94*, 8168–8172.

704 Sternberg, S.H., Redding, S., Jinek, M., Greene, E.C., and Doudna, J.A. (2014). DNA interrogation
705 by the CRISPR RNA-guided endonuclease Cas9. Nature *507*, 62–67.

706 Tan, S.Z., Reisch, C.R., and Prather, K.L.J. (2018). A Robust CRISPRi Gene Repression System
707 inPseudomonas. J. Bacteriol. *200*, e00575-17.

708 Teufel, R., Mascaraque, V., Ismail, W., Voss, M., Perera, J., Eisenreich, W., Haehnel, W., and
709 Fuchs, G. (2010). Bacterial phenylalanine and phenylacetate catabolic pathway revealed. Proc.
710 Natl. Acad. Sci. U. S. A. *107*, 14390–14395.

711 Tomich, M., Herfst, C.A., Golden, J.W., and Mohr, C.D. (2002). Role of flagella in host cell
712 invasion by Burkholderia cepacia. Infect. Immun. *70*, 1799–1806.

713 Vigouroux, A., Oldewurtel, E., Cui, L., Bikard, D., and Teeffelen, S. van (2018). Tuning dCas9's
714 ability to block transcription enables robust, noiseless knockdown of bacterial genes. Mol. Syst.
715 Biol. *14*, e7899.

Table 1. Putative host range of the mini-CTX system and genomic context of selected hit sites

Class	Order	Family	Genus and Species	Strain	%GC	tRNA^{Ser} ( ) Genomic Context
Gammaproteobacteria	Pseudomonadales	Pseudomonadaceae	*Pseudomonas aeruginosa*	PAO1	66.6	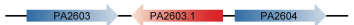
			Pseudomonas fluorescens	NCTC 10783	65.9	
			Pseudomonas mendocina	NK-01	64.7	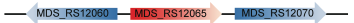
		Moraxellaceae	*Acinetobacter baumannii*	ATCC 17978	39	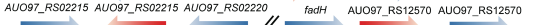
			Acinetobacter nosocomialis	NCTC 8102	38.7	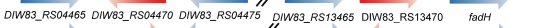
	Xanthomonadales	Xanthomonadaceae	*Xylella fastidiosa*	M12	51.9	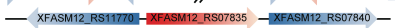
Betaproteobacteria	Burkholderiales	Alcaligenaceae	*Achromobacter xylosoxidans*	NCTC 10808	67.4	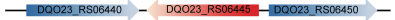
			Bordatella bronchiseptica	D448	68.1	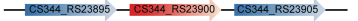
			Alcaligenes faecalis	DSM 30030	56.6	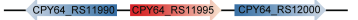
		Burkholderiaceae	*Ralstonia pickettii*	DTP0602	65.9	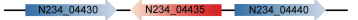
			Burkholderia cenocepacia	K56-2	67	
			Burkholderia multivorans	ATCC 17616	66.7	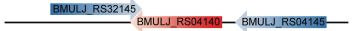
			Burkholderia thailandensis	E264	67.7	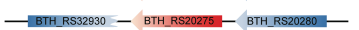
			Burkholderia mallei	NCTC 10229	68.5	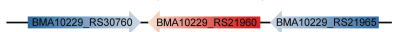
			Burkholderia pseudomallei	NCTC 13178	67.9	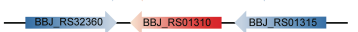
			Burkholderia oklahomensis	EO147	66.9	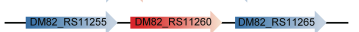
			Cupriavidus necator	NH9	65.5	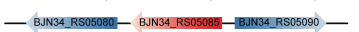
			Pandoraea apista	AU2161	62.6	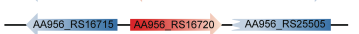
			Lautropia mirabilis	NCTC 12852	65.5	
		Oxalobactericeae	*Collimonas fungivorans*	Ter6	59	
		Commamonadaceae	*Rhodoferax antarcticus*	DSM 24876	58.9	
			Polaromonas naphthalenivorans	CJ2	61.7	
	Neisseriales	Neisseriaceae	*Neisseria meningitidis*	NCTC 10026	51.4	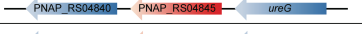
			Neisseria gonorrheae	NCTC 13484	52.5	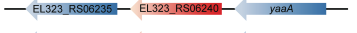
			Neisseria sicca	FDAARGOS_260	50.9	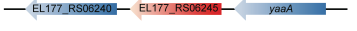
			Chromobacterium violaceum	CV1197	65.6	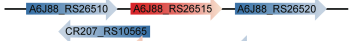
	Nitrosomonadales	Nitrosomonadaceae	*Nitrosomonas communis*	Nm2	44.7	
Hydrogenophilalia	Hydrogenophilales	Hydrogenophilaceae	*Hydrogenophilus thermoluteolus*	TH-1	61.7	
Alphaproteobacteria	Rhodospirillales	Rhodospirillaceae	*Haematospirillum jordaniae*	H5569	55.6	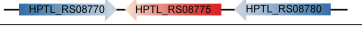

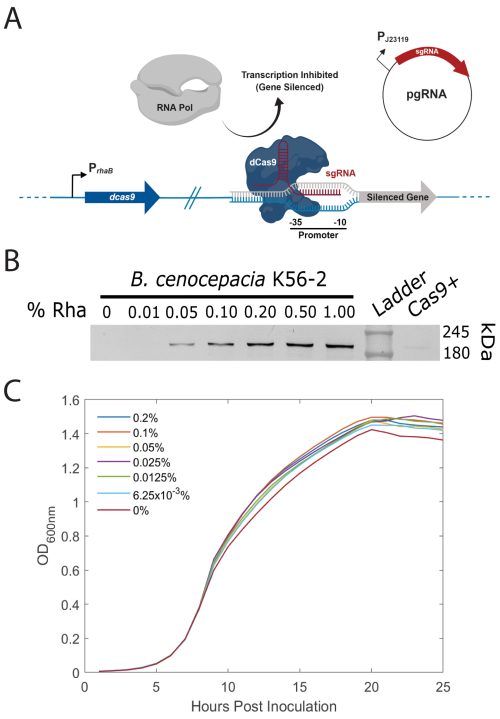

Figure 1. Development of CRISPRi in *B. cenocepacia* K56-2. A) The CRISPRi toolkit is composed of a chromosomal codon-optimized version of the *S. pyogenes dcas9* and plasmid pgRNA harboring the sgRNA under the control of the constitutive promoter P_{J23119}. B) dCas9 is dynamically expressed from the chromosome of K56-2 by rhamnose. Cells were grown to OD_{600nm} of 0.6 then induced with rhamnose for three hours. Soluble protein was harvested and run on an 8% SDS gel. dCas9 was detected by an α-dCas9 antibody then by a 2° antibody linked to alkaline phosphatase C) Chromosomally-encoded dCas9 induced with rhamnose up to 0.2% does not affect growth in K56-2.

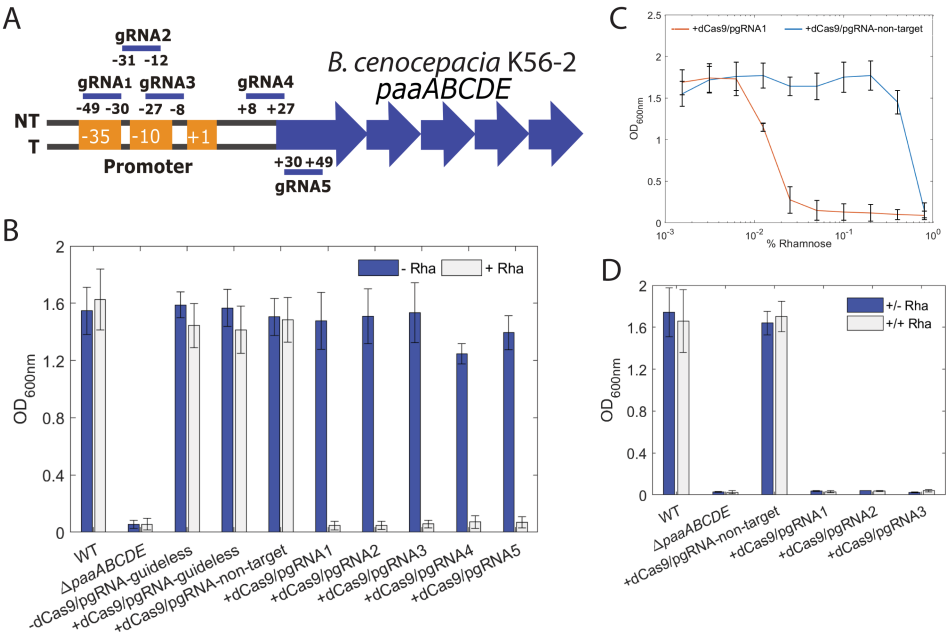

Figure 2. Targeting *paaA* with CRISPRi effectively suppresses growth in phenylacetic acid as the sole carbon source in *B. cenocepacia* K56-2. A) Positions of the sgRNAs targeting different regions upstream of and on *paaA*. sgRNAs 1, 2, and 3 were designed to target the promoter elements (-35 and -10 boxes) on the non-template (NT) strand. gRNA4 targeted the start codon on the NT strand and gRNA5 targeted the downstream region adjacent to the start codon on the T strand. B) CRISPRi blocks transcription in a strand non-specific manner. WT, a mutant of the *paaABCDE* operon (Δ*paaABCDE*), K56-2::CTX1-rha (-dCas9) and K56-2::dCas9 (+dCas9) harboring pgRNA with or without specific gRNAs were grown for 24 hours in minimal medium with PA (M9+PA) without (-Rha) or with 0.2% rhamnose (+Rha). C) Expression of the dCas9 can be controlled by varying the amount of inducer added to the medium, providing tunability to the CRISPRi system. However, high level induction of dCas9 with rhamnose (0.4% and beyond) was lethal for the non-genome targeting mutant expressing dCas9. D) Cells were grown overnight in LB medium with 0.2% rhamnose to induce expression of dCas9. Then cells were transferred to fresh medium and grown with (+/+ Rha) and without (+/- Rha) 0.2% rhamnose. All the values are the average of three independent biological replicates; error bars represent arithmetic mean ± SD.

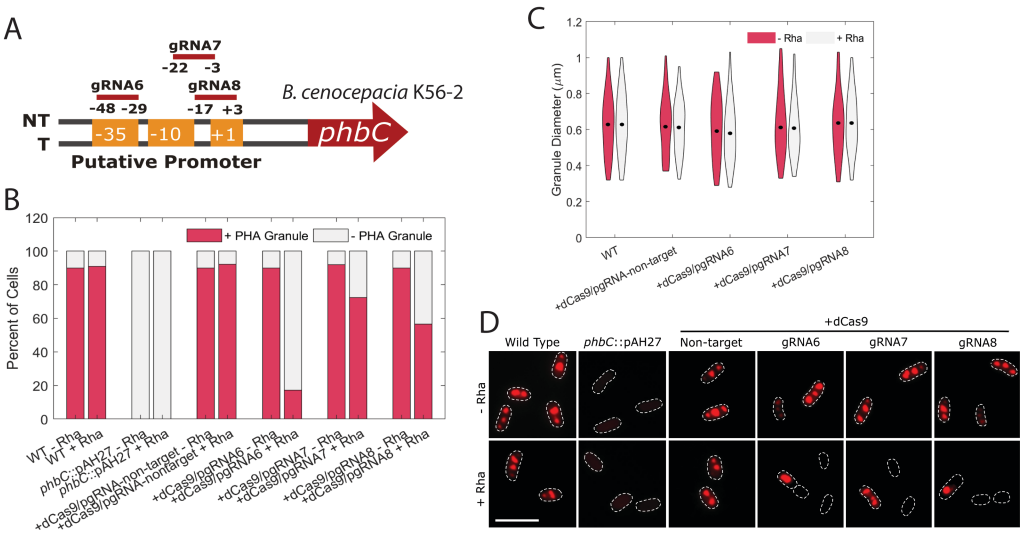

Figure 3. Targeting *phbC* with CRISPRi reduces polyhydroxyalkanoate (PHA) granule accumulation in K56-2. A) Positions of the sgRNAs targeting different regions upstream of *phbC*. sgRNAs 6, 7, and 8 were designed to target the promoter elements (-35 and -10 boxes) on the non-template (NT) strand. B) CRISPRi reduces but does not completely abrogate the number of cells with PHA granules. WT, an insertional mutant of the *phbC* gene (*phbC*::pAH27), K56-2::CTX1-rha (-dCas9) and K56-2::dCas9 (+dCas9) harboring pgRNA with or without specific gRNAs were grown overnight without (-Rha) or with 0.2% rhamnose (+Rha). Cells were washed and stained with Nile Red, and observed by fluorescence microscopy. One to two-hundred cells were counted and the % of cells with PHA granules was calculated. C) PHA granules that remain are identical to those in the WT. Strains were grown and processed as for B and the diameter of the PHA granules was measured. Thicker areas of the violin bars represent more granules with that diameter. The mean in each condition is shown by a black dot. D) The strains were grown and processed as for B). Dashes indicate cell boundaries and the scale bar is 5 μm.

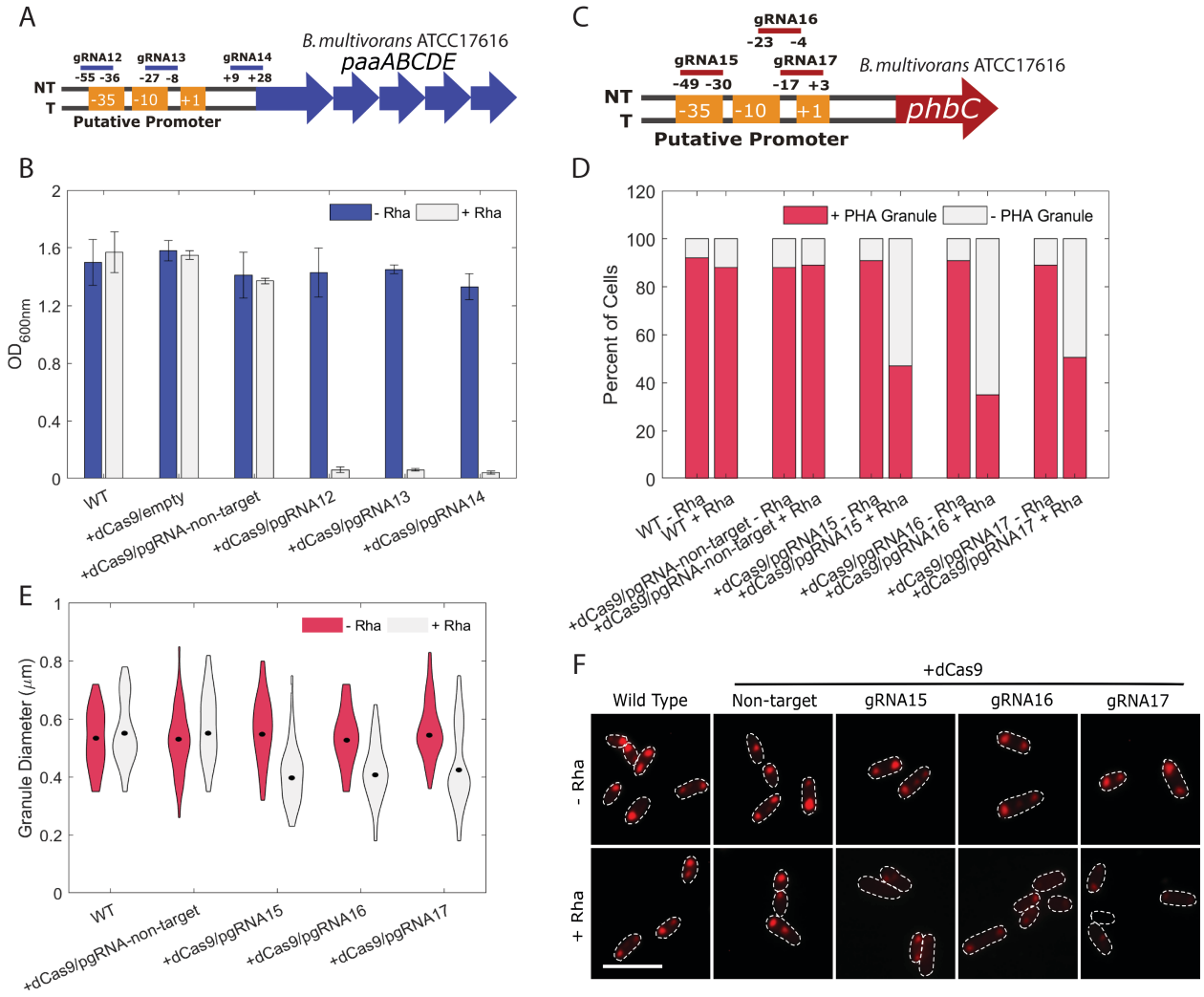

Figure 4. CRISPRi in *B. multivorans* ATCC17616 effectively represses *paaA* and *phbC*. A) Positions of the sgRNAs targeting upstream regions of *paaA*. sgRNAs 12 and 13 were designed to target the -35 and -10 boxes of the promoter, while sgRNA14 targeted the 5' region of the ORF. All sgRNAs targeted the NT strand. B) Targeting *paaA* suppressed growth on PA as a sole carbon source. WT, ATCC 17616::dCas9 (+dCas9) with or without sgRNAs in A) were grown for 24 hours in M9+PA without (-Rha) or with 0.2% rhamnose (+Rha). C) Positions of the sgRNAs targeting upstream regions of *phbC*. All sgRNAs were designed to target the -35 or -10 elements of the promoter on the NT strand. D) Targeting *phbC* reduces the overall number of cells with

773 PHA granules. Strains were grown overnight without (-Rha) or with 0.2% rhamnose (+Rha). Cells
774 were washed and stained with Nile Red, and observed by fluorescence microscopy. One to two-
775 hundred cells were counted and the % of cells with PHA granules was calculated. E) PHA granules
776 that remain are smaller than those in the WT. Strains were grown and processed as for D); however,
777 the diameter of the PHA granules was measured, with thicker areas representing more granules
778 with that diameter. The mean in each condition is shown by a black dot. F) The strains were grown
779 and processed as for D). Dashes indicate cell boundaries and the scale bar is 5 μm.

780

781

782

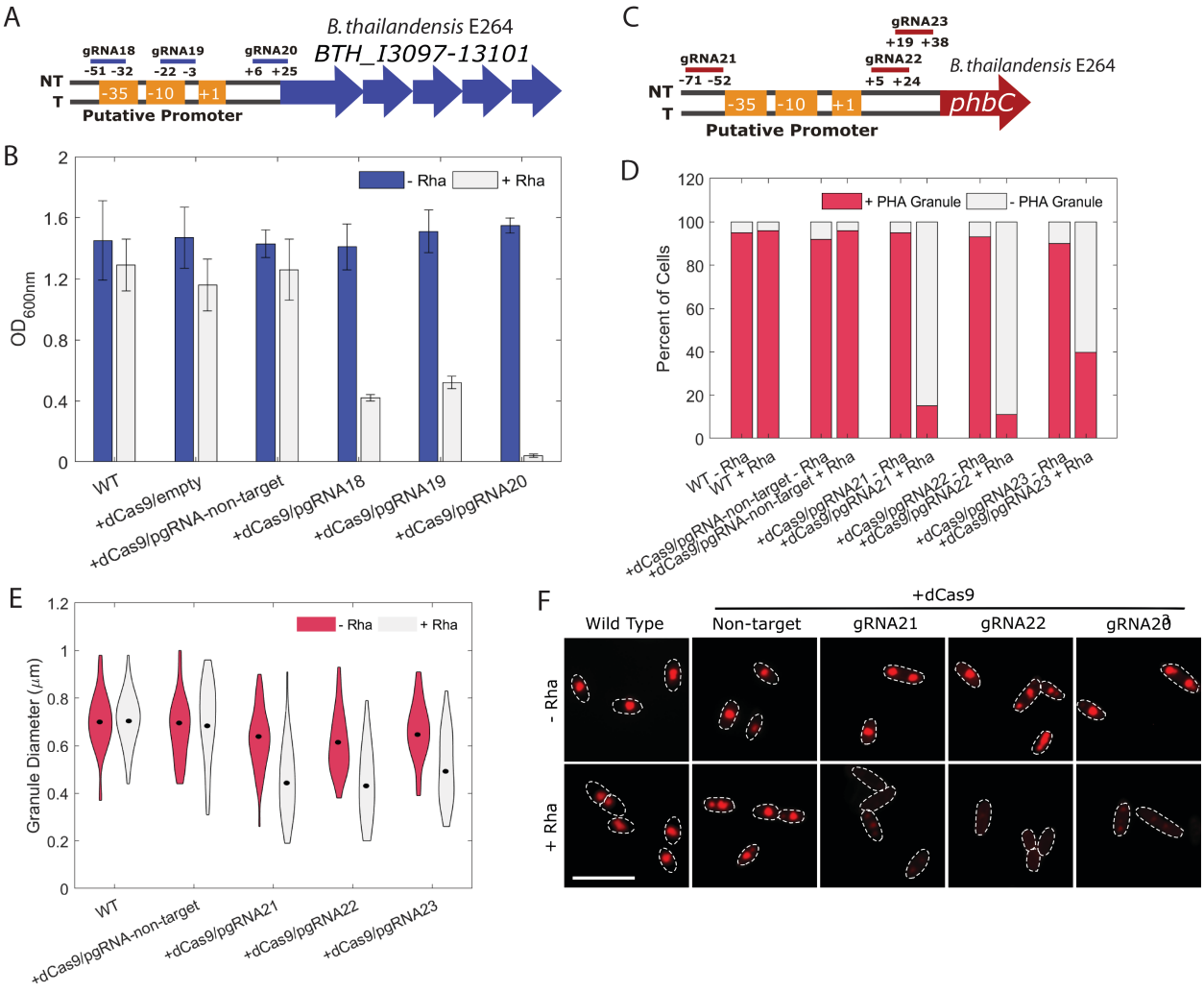

Figure 5. CRISPRi in *B. thailandensis* E264 effectively represses *paaA* (BTH_I3097) and *phbC*. Positions of the sgRNAs targeting upstream regions of *paaA* (BTH_I3097). sgRNAs 18 and 19 were designed to target the -35 and -10 boxes of the promoter, while sgRNA 20 targeted the 5' region of the ORF. All sgRNAs targeted the NT strand. B) Targeting *paaA* suppressed growth on PA as a sole carbon source. WT, E264::dCas9 (+dCas9) with or without sgRNAs in A) were grown for 48 hours in M9+PA without (-Rha) or with 0.2% rhamnose (+Rha). C) Positions of the sgRNAs targeting regions of *phbC*. sgRNA 21 targeted just upstream of the -35 box, sgRNA22 and 23 targeted just downstream of the -10 box, all on the NT strand. D) Targeting *phbC* reduces the

overall number of cells with PHA granules. Strains were grown overnight without (-Rha) or with 0.2% rhamnose (+Rha). Cells were washed and stained with Nile red, and observed by fluorescence microscopy. One to two-hundred cells were counted and the % of cells with PHA granules was calculated. E) PHA granules that remain are smaller than those in the WT. Strains were grown and processed as for D); however, the diameter of the PHA granules was measured, with thicker areas representing more granules with that diameter. The mean in each condition is shown by a black dot. F) The strains were grown and processed as for D). Dashes indicate cell boundaries and the scale bar is 5 μm.